17th World Conference on Earthquake Engineering, 17WCEE
Sendai, Japan - September 13th to 18th 2020

EXPERIMENTAL EVALUATION OF STRUCTURAL BEHAVIOR OF RC FRAMES WITH BRACE HAVING FRICTION DAMPER

Y. Maida(1), K. Kasai(2), H. Sakata(3)

(1) *Senior Researcher, Building Dept., National Institute for Land and Infrastructure Management, maida-y92gy@mlit.go.jp*
(2) *Specially Appointed Prof., FIRST, Tokyo Institute of Technology, kasai.k.ac@m.titech.ac.jp*
(3) *Prof., Dept. of Arch. and Build. Eng., Tokyo Institute of Technology, sakata.h.aa@m.titech.ac.jp*

Abstract

Friction damper have been used as energy-dissipating devices to retrofit existing reinforced concrete (RC) frames in Japan. Some effort has also been devoted to applications of friction dampers in newly-built RC moment-resisting frames, where efficient and reliable connections between dampers and concrete components become an important issue. In addition, the beam in the RC frames with the damper is acted the horizontal force of the damper as an axial force.

In this paper, cyclic loading test of RC frames with brace having friction damper was adopted the boundary condition that can reproduce axial force to act on a beam and confirmed the effectiveness of a new connection method. In order to resist the axial force acting on the RC member, a damper connection method is proposed in which a steel material attaching ed through the center of the RC member. In this connection method, most of the axial forces are resisted by steel material (steel plate or deformed bar) through the beam and column section inside. This test is conducted to evaluate the behavior of the proposed damper connections and its influence to the surrounding components.

Each specimen consists of a one story and one span RC frame into one brace having friction damper that are diagonally connected to the RC joint. The steel plate with the gusset plate is embedded in RC joint to connect a damper. Five specimens were tested. These were ‘CP series’ of steel plate through the RC frame inside; ‘NP series’ of steel material not through the RC frames inside. In the above two series specimens, the stud bolts was welded to the embedded plate to resist the damper force. In the three specimen series, namely ‘CD series’ in which deformed bar through the RC frame inside. The parameter is with or without brace having damper in NP and CD series. CP series specimen tested only without brace having damper.

In loading, at first, the stub of the specimen fixed to the reaction frame. The jack is connected with the center of the beam as the pin support. In order to reproduce the axial force acting on the beam, a jack is connected with the center of the beam as a pin support. The horizontal force is applied by jacks connected from the reaction frame on both sides.

From the test results, friction damper deformation loss is dominated by the axial deformation of the beam rather than the deformation of the damper connection. The test results indicate that the influence of the deformation loss in the connection on the performance of the friction dampers is negligible. By arranging the deformed reinforcing bar in the center of the cross section of the beam member, axial deformation of the beam can be suppressed, and the damper can secure stable hysteresis characteristics. In addition, it was confirmed that the crack of the RC beam and column occurred small in CP and CD series specimen even if an axial force due to the damper acted.

Keywords: RC frames; friction damper; steel plate; stud bolts; deformed bar

1. Introduction

Friction dampers have stable hysteresis characteristics and are effective for ensuring the earthquake resistance of reinforced concrete (RC) frames. However, it is necessary to consider that the horizontal component of the damper force acts on the beam as an axial force. Based on the above, a cyclic loading test of RC frames with brace having friction damper using the new connection method is conducted. From the test, the behavior of the damper connection and RC frame is grasped.

2. Outline of the test

2.1 Specimens

Table 1 shows the specifications of the specimen. Tables 2 and 3 show the material properties of concrete and rebar. Fig. 1 shows the details of the RC specimen. Fig. 2 shows the details of the damper.

The specimen was a 1-story, 1-span RC frames consisting of approximately 1/3 scale columns and beams for the lowest story of a 7-story RC building designed for trial in “AIJ Standard for Structural

Table 1 – Specimen properties

			CP-N	NP-N	CD-N	NP-D	CD-D
Center of the members			Steel Plate	-	Deformed bar	-	Deformed bar
Stud bolts			16-φ9.5 (beam) 8- φ9.5 (column)		-	16-φ9.5 (beam) 8- φ9.5 (column)	-
Damper			-			Yes	
Column	Dimensions[mm]		320×320				
	Fc[N/mm^2]		27				
	Rebar		12-D13 (SD390) p_t=0.50%				
	Hoop		4-D6@70 (USD785) p_w=0.57%				
	Axial force [kN]		461				
Beam	Dimensions[mm]		130×280				
	Fc[N/mm^2]		27				
	Rebar	Top	3+2-D10 (SD390) p_t=0.98%				
		Bottom	3+2-D10 (SD390) p_t=0.98%				
	Stirrup		3-D6@60 (USD785) p_w=1.23%				
Stub	Dimensions[mm]		360×500				
	Fc[N/mm^2]		27				
	Rebar	Top	4-D22 (SD345) p_t=0.86%				
		Bottom	2+4-D22 (SD345) p_t=1.29%				
	Stirrup		4-D13@70 (SD345) p_w=2.02%				

Fc: Design strength of concrete

© The 17th World Conference on Earthquake Engineering

Table 2 – Material properties of concrete

	Column, beam			Stub		
	σ_B	σ_T	E_C	σ_B	σ_T	E_C
CP-N	32.9	2.5	2.47	27.1	2.2	2.01
NP-N	33.8	2.8	2.41	27.9	2.5	2.16
CD-N	39.0	2.9	2.87	37.8	2.8	2.61
NP-D	42.1	3.5	2.91	40.3	3.0	3.12
CD-D	38.5	2.6	2.63	37.4	2.2	2.59

σ_B: Concrete compressive strength, σ_T: Concrete tensile strength, E_C: Concrete elastic modulus

Table 3 – Material properties of rebar

	Column rebar			Beam rebar			Hoop, stirrup			Stub rebar			Stub stirrup		
	D13 (SD390)			D10 (SD390)			U6 (USD785)			D22 (SD345)			D13 (SD345)		
	σ_y	σ_u	E_S	σ_y	σ_u	E_S	σ_y	σ_u	E_S	σ_y	σ_u	E_S	σ_y	σ_u	E_S
CP-N NP-N	420	611	1.94	451	651	1.91	959*	1184	1.91	384	555	1.79	402	556	2.00
CD-N NP-D CD-D	419	613	1.92	435	627	2.02	956*	1165	1.90	384	520	1.78	359	540	1.89

σ_y: Yield strength, σ_u: Tensile strength, E_S: Young's modulus, *0.2% proof stress

Calculation of Reinforced Concrete Structures" [1]. The axial force ratio of the column was set to 0.15, and the axial force was applied by an unbonded PC steel rod. A steel plate with a gusset plate (G.PL) was embedded in the beam-column joint to connect the damper. The damper mounting angle α was set at 26.1°, and the force in the damper was set at 236 kN so that the ratio of the horizontal component to the calculated yield strength of the RC frames was approximately 1: 1. The maximum sliding distance of the damper was designed to be ± 50mm.

Five specimens were tested. These were 'CP series' of steel plates through the RC frame inside; 'NP series' of steel material not through the RC frames inside. In the above two series specimens, the stud bolts was welded to the embedded plate to resist the force in the damper. In the third specimen series, namely 'CD series' in which deformed bars through the RC frame inside to resist the force in the damper. The parameter is with or without brace having damper in NP and CD series. CP series specimen tested only without brace having damper. The steel plates and deformed bars inside the beams of the CP and CD series were designed to remain within the elastic range for the horizontal component of the force in the damper. It is expected that the concrete cracks will close after unloading if the steel inside the RC member is in the elastic range. Both the inside of the column and the beam were set to PL-14 × 111 (SN400) for the CP series specimen and D25 (SD490) for the CD series specimen. Stud bolts to be welded to steel plates in the CP and NP series were designed based on "Design Recommendations for Composite Structures" [2] for the force in the damper. The horizontal component (170kN) of the force in the damper was borne by stud bolts on the beam side, and the vertical component (83kN) was borne by stud bolts on the column side. The stud bolts used 16-ϕ9.5 on the beam side and 8- ϕ9.5 on the column side. The embedded length of the stud bolts was 50 mm.

© The 17th World Conference on Earthquake Engineering

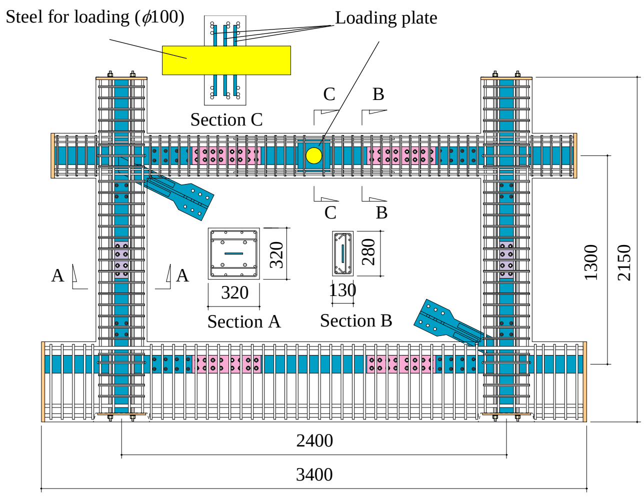

(a) CP series

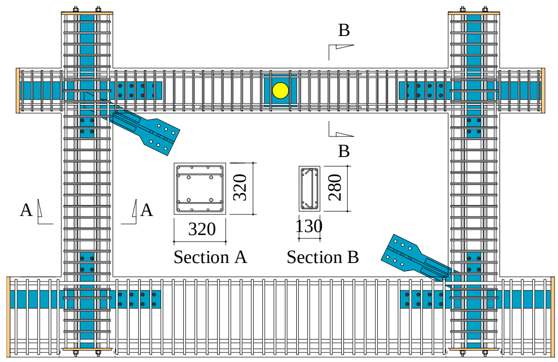

(b) NP series

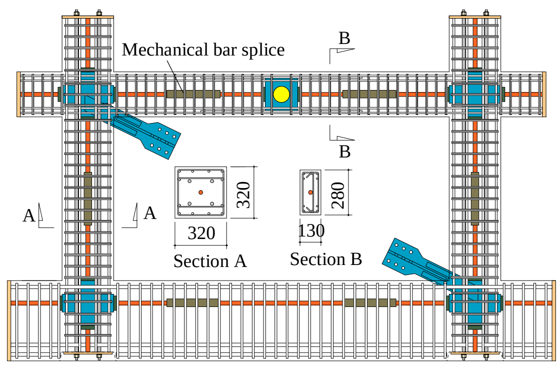

(c) CD series

Fig. 1 – Details of RC frame (Unit: mm)

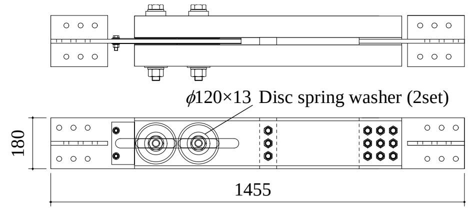

Fig. 2 – Details of damper (Unit: mm)

© The 17th World Conference on Earthquake Engineering

2.2 Loading

Fig. 3 shows the test setup. In loading, at first, the stub of the specimen fixed to the reaction frames. In order to reproduce the axial force acting on the beam, a jack is connected with the center of the beam as a pin support. The horizontal force is applied by jacks connected from the reaction frame on both sides. At the time of positive load, the left jack in the figure was controlled for tensile displacement, and the right jack maintained zero load. At the time of negative force, the reverse force was applied.

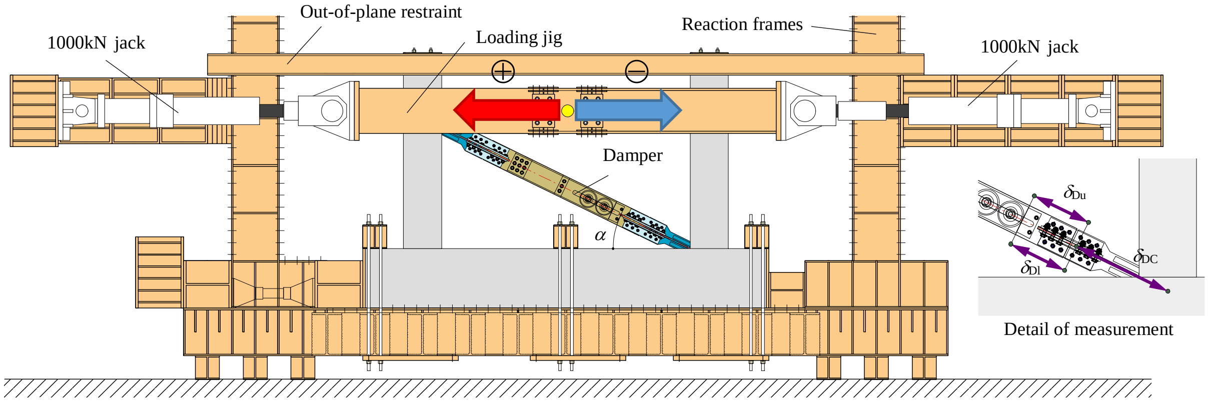

Fig. 3 – Test setup and measurement

3. Test result

3.1 Story drift ratio-story shear force relation

Fig. 4 shows the story drift ratio R versus story shear force Q relationship. The story shear force of the whole system Q_S is the sum of the shear force of the RC frame Q_F and the horizontal component of the axial force in the damper Q_D. Fig. 4 shows the story shear force of the whole system separated into the force of the RC frame and the damper.

In CP-N, NP-N and CD-N without damper, all specimens had stable hysteresis characteristics up to R = 1/33rad. It was confirmed that the ultimate failure mode was flexural failure of the beam and no brittle failure occurred. The maximum strength was 519kN for CP-N, 421kN for NP-N, and 490kN for CD-N. In NP-D with a damper had a stable hysteresis characteristic up to R = 1/33 rad. The ultimate failure mode was flexural failure of the beam. In CD-D, the story shear force was reduced at the time of R = 1/50 rad cycle, but the axial force was still stable with the damper, and the rigidity of the RC frame slightly decreased on the negative load side. As a cause of the decrease in story shear force, it was confirmed that the weld between the steel plate with G.PL and the deformed bar in the beam-column joint after the test.

3.2 Damages of the RC frames

Fig. 5 shows the damages of the RC frames at R = ± 1/100rad. In all specimens, flexural cracks in beams and column bases were confirmed at R = 1/800 or 1/400 rad. No shear crack occurred at the beam-column joint until the end of the test.

In the CP and CD series, maximum crack was confirmed near the critical section in the beam, while in the NP series, maximum crack was confirmed at the position where the steel plate inside the beam was interrupted. The hinge position changed depending on the presence or absence of the internal steel member.

3.3 Behavior of sliding part of the damper

Fig. 6 shows the axial force in the damper N_D versus the sliding displacement of the damper δ_D relationship. For both NP-D and CD-D, the damper had stable hysteresis characteristics until the end of the test. However,

© The 17th World Conference on Earthquake Engineering

at the time of large deformation of R = 1/100, 1/50, 1/33rad cycle, there was a difference in the sliding displacement of the damper between the tension side and the compression side. This is considered to be due to the influence of the axial deformation of the beam.

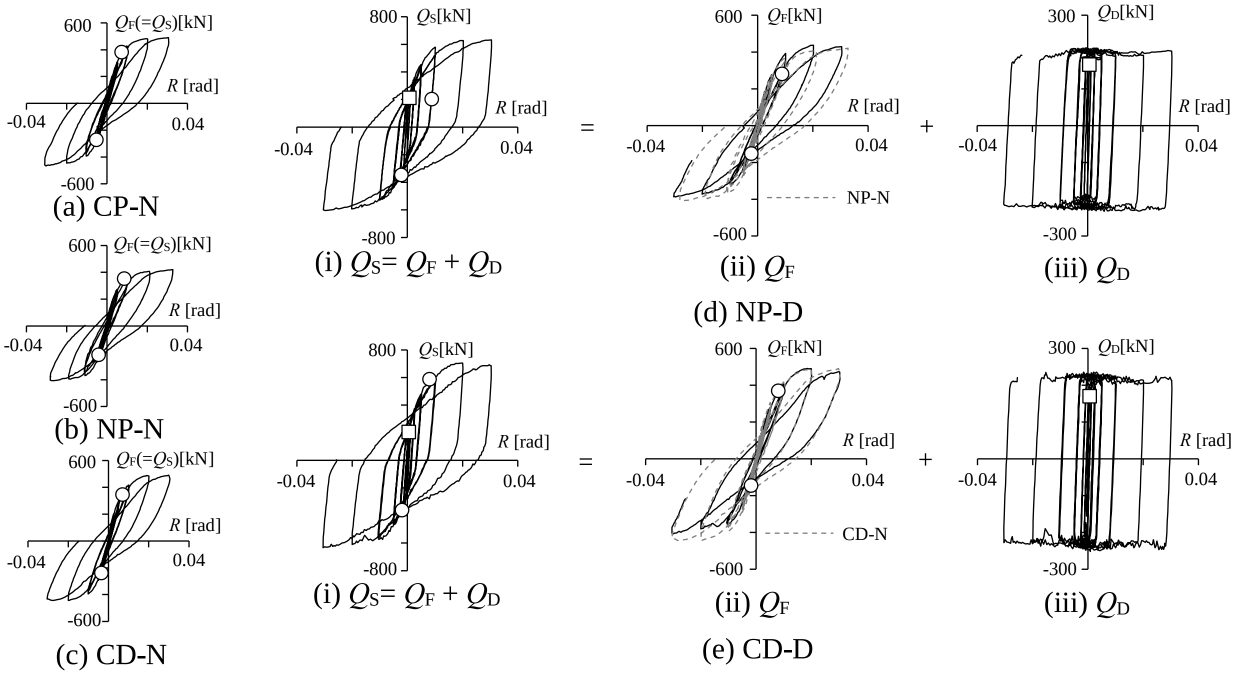

○: Rebar yields, □: Damper's sliding force reaches

Fig. 4 – Story drift ratio R versus story shear force Q relationship

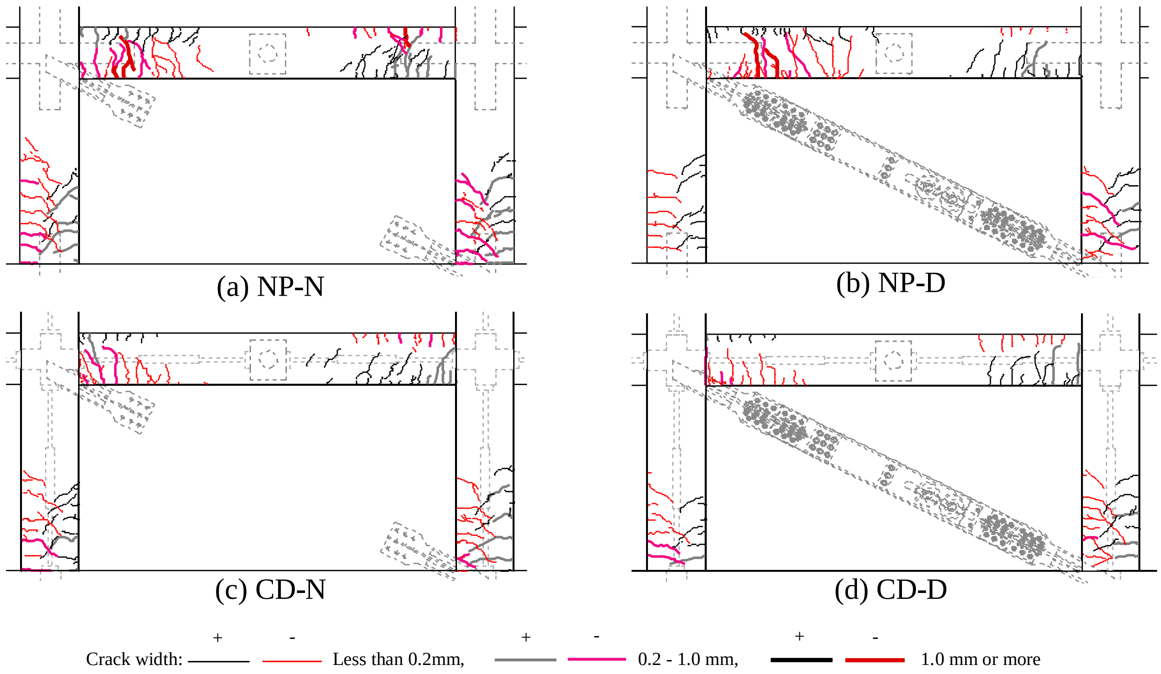

Fig. 5 – Damages of the RC frames at $R = \pm$ 1/100rad

© The 17th World Conference on Earthquake Engineering

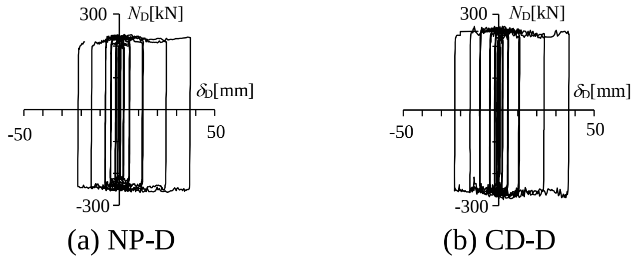

Fig. 6 – Axial force in the damper N_D versus the sliding displacement of the damper δ_D relationship

3.4 Axial deformation of the beam

Fig. 8 shows the story shear force Q_F versus the axial deformation on the left side of the beam δ_{GL} relationship in the specimen without damper. The axial deformation of the beam was measured as a relative displacement near the center of the beam and to the column center, including the deformation of a part of the beam-column joint, as shown in Fig. 7.

The axial deformation on the left side of the beam is up to approximately 5 mm for CP-N and CD-N. On the other hand, in the NP-N test specimen, axial deformation on the left side of the beam occurred more than 8 mm. It was confirmed that axial deformation of the beam can be suppressed by passing a steel member inside the beam.

Next, the axial deformation on the left side of the beam δ_{GL} versus the sliding displacement of the damper δ_D relationship is considered in the CD-D. In Fig. 9, the vertical axis shows the axial force in the damper N_D, and the horizontal axis shows the axial deformation on the left side of the beam δ_{GL} and the sliding displacement of the damper δ_D. The bold line indicates the R = -1 / 50 rad cycle. When the deformed bar inside the beam breaks and the axial deformation of the beam increases, the sliding displacement of the damper decreases. Therefore, passing a deformed bar through the beam is effective to secure a stable sliding displacement of the damper.

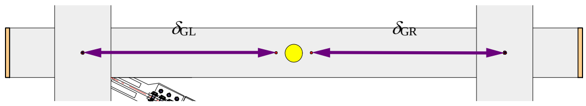

Fig. 7 – Measurement of axial deformation of the beam

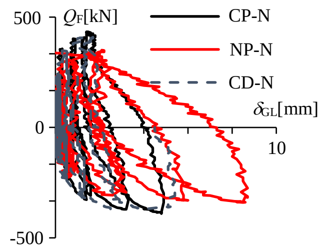

Fig. 8 – Story shear force Q_F versus the axial deformation on the left side of the beam δ_{GL} relationship

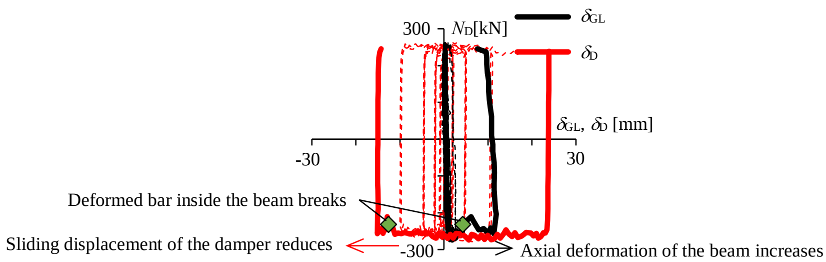

Fig. 9 – Axial deformation of the beam δ_{GL} and the sliding displacement of the damper δ_D

© The 17th World Conference on Earthquake Engineering

3.5 Loss of sliding displacement of the damper

The axial deformation of the beam and the axial deformation of the damper connection are considered focusing on the force in the damper. As shown in Fig. 10 (i), regarding the damper in the axial force at the R = -1/100 rad cycle, the behavior in each state of transition from tension to compression (thick black line), constant compression (thick red line), and transition from compression to tension (thick blue line) is considered. The vertical axis in Fig. 10 is the shear force of the RC frame Q_F in the left diagram and the damper in the axial force N_D in the right diagram.

From the damper in the axial force N_D versus the sliding displacement of the damper δ_D relationship shown in Fig. 10 (i), the sliding displacement of the damper of -7.5mm and -9.7mm was confirmed for NP-D and CD-D at the peak of R = -1/100rad. By passing the deformed bar inside the beam, a stable sliding displacement of the damper was secured.

Fig. 10 (ii) shows the axial deformation on the left side of the beam δ_{GL}. In the NP-D, axial deformation on the left side of the beam δ_{GL} is approximately 2 mm during the elastic range. When the beam yields, it increases to approximately 8mm at the peak of R = -1/100rad. On the other hand, in the CD-D, even after the beam yielded, the axial deformation o n the left side of the beam δ_{GL} was suppressed to approximately 2 mm even at the peak of R = -1/100 rad due to the presence of the deformed bar inside the beam.

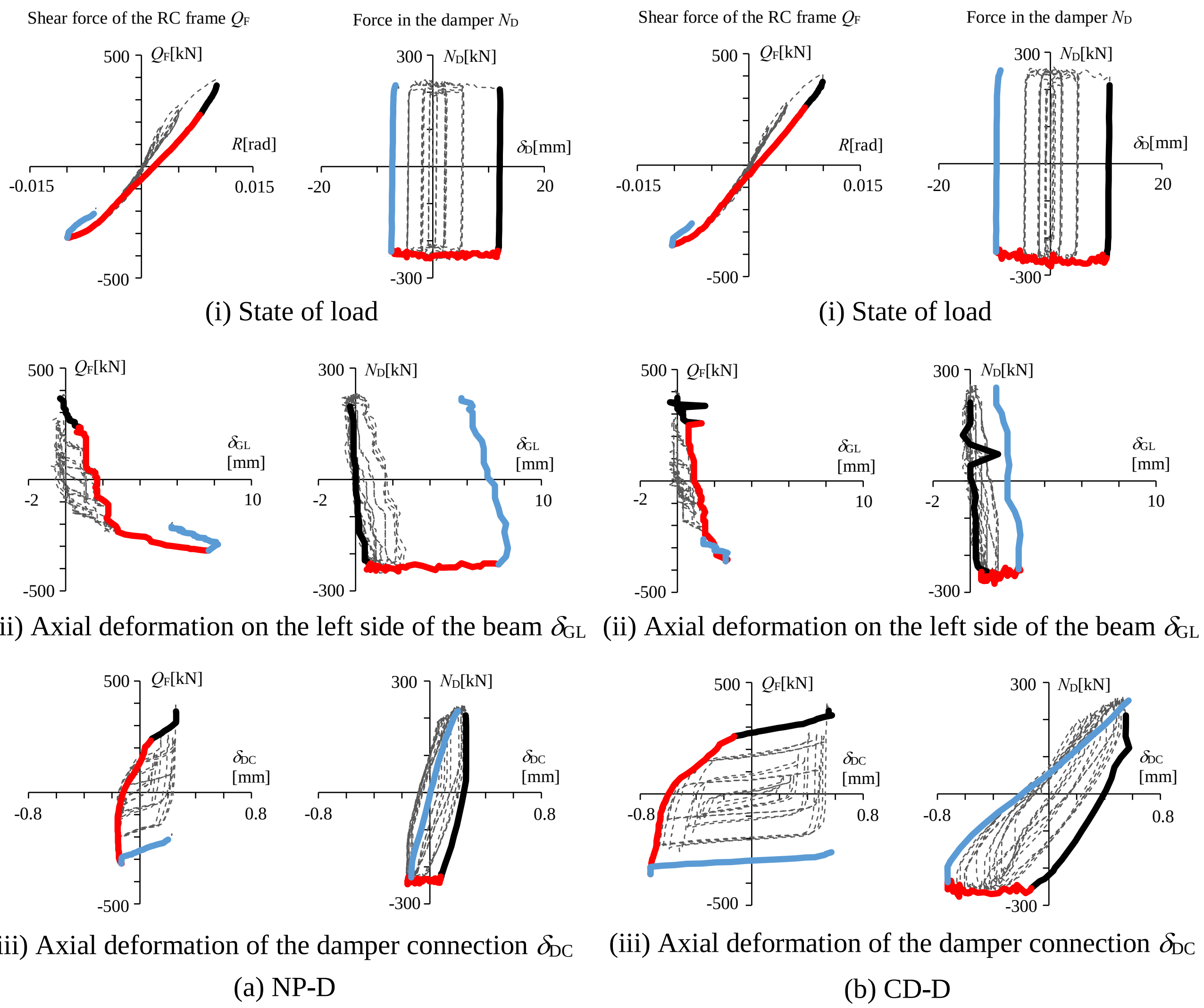

Fig. 10 – Axial deformation of the beam δ_{GL} and the axial deformation of the damper connection δ_{DC}

© The 17th World Conference on Earthquake Engineering

Fig. 10 (iii) shows the axial deformation of the damper connection δ_{DC}. In all the specimens, the axial deformation of the damper connection δ_{DC} changes when the damper axial force shifts, indicating that the influence of the shear force of the RC frame Q_F is small. The maximum the axial deformation of the damper connection δ_{DC} occurred approximately 0.2 mm in NP-D and approximately 0.75 mm in CD-D up to R = -1/100 rad. When the maximum axial deformation on the left side of the beam δ_{GL} described above is converted into the axial component of the brace, it is approximately 8.7 mm in NP-D and approximately 2.2 mm in CD-D. Therefore, the loss of sliding displacement of the damper is less affected by the axial deformation of the damper connection, and the loss by the axial deformation of the beam is dominant.

3.6 Behavior of stud bolts

Next, the behavior of the stud bolts will be considered. Focus on the horizontal curvature hysteresis of the S12 and S42 stud bolts shown in Fig. 11. In Fig. 12(a), the vertical axis represents the shear force of the RC frame Q_F, and the horizontal axis represents the horizontal curvature of the stud bolts ϕ_{SH}. Fig. 12 (b) shows the S42 stud bolt in the NP-D for each load state of the axial force in the damper as in section 3.5.

According to Fig. 12 (a), regardless of the presence or absence of the damper, the curvature is larger in S42 than in S12. In NP-N, the curvature on the positive side occurs, but in NP-D, the curvature on the negative side occurs when the positive loading, and the curvature on the positive side occurs when the negative loading. Therefore, it can be seen that the stud bolt bears the force in the damper.

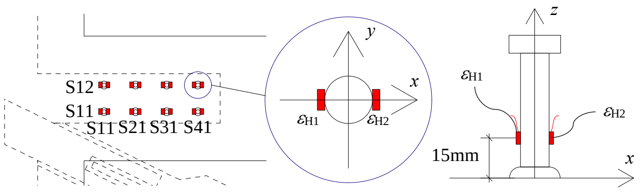

Fig. 11 – Strain gauge sticking position of stud bolts

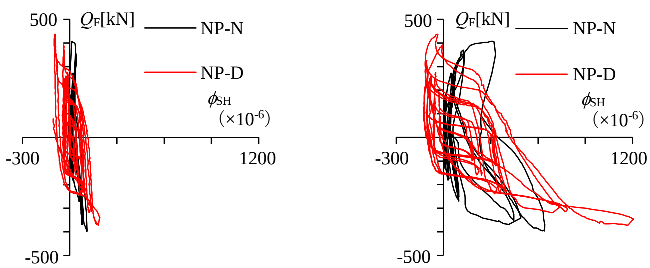

(i) S12 (ii) S42

(a) Comparison of NP-N and NP-D

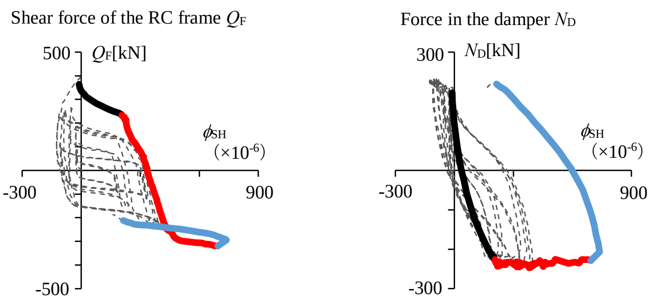

(b) S42 stud bolt in the NP-D

Fig. 12 – Curvature hysteresis of the stud bolts

© The 17th World Conference on Earthquake Engineering

According to Fig. 12 (b), the curvature does not increase so much when the axial force in the damper shifts from tension to compression, but increases when the RC frame yields and the shear force of the RC frame gradually increases. Also, when the force in the damper shifts from compression to tension, the curvature decreases significantly.

4. Conclusions

In this paper, the structural behavior of RC frames with brace having friction damper was confirmed by cyclic horizontal loading test. The results obtained are summarized below.

- Both the method of embedding the G.PL with stud bolts near the beam-column joint and the method of passing the deformed bar through the inside the RC member are effective for application the damper in the RC frames.
- The loss of sliding displacement of the damper is less affected by the axial deformation of the damper connection, and the loss by the axial deformation of the beam is dominant. However, by passing the deformed bar inside the beam, axial deformation of the beam can be suppressed, and a stable sliding displacement of the damper can be secured.

5. Acknowledgements

This work was supported by Grant-in-Aid for Scientific Research (A), JSPS KAKENHI Grant Number 23246098. In the test, friction damper was provided by OBAYASHI CORPORATION. These support is gratefully acknowledged.

6. References

[1] Architectural Institute of Japan (2010): AIJ Standard for Structural Calculation of Reinforced Concrete Structures (in Japanese)

[2] Architectural Institute of Japan (2010): Design Recommendations for Composite Structures (in Japanese)

© The 17th World Conference on Earthquake Engineering